Quantum Transport and Magnetism of Dirac Electrons in Solids

Hiroki Isobe[1] and Naoto Nagaosa[2,1]

[1]*Department of Applied Physics, University of Tokyo, Bunkyo, Tokyo, 113-8656 Japan*
[2]*RIKEN Center for Emergent Matter Science (CEMS), Wako, Saitama 351-0198, Japan*

The relativistic Dirac equation covers the fundamentals of electronic phenomena in solids and as such it effectively describes the electronic states of the topological insulators like Bi_2Se_3 and Bi_2Te_3. Topological insulators feature gapless surface states and, moreover, magnetic doping and resultant ferromagnetic ordering break time-reversal symmetry to realize quantum anomalous Hall and Chern insulators. Here, we focus on the bulk and investigate the mutual coupling of electronic and magnetic properties of Dirac electrons. Without carrier doping, spiral magnetic orders cause a ferroelectric polarization through the spin-orbit coupling. In a doped metallic state, the anisotropic magnetoresistance arises without uniform magnetization. We find that electric current induces uniform magnetization and conversely an oscillating magnetic order induces electric current. Our model provides a coherent and unified description of all those phenomena. The mutual control of electric and magnetic properties demonstrates implementations of antiferromagnetic spintronics. We also discuss the stoichiometric magnetic topological insulator $MnBi_2Te_4$.

Relativistic effects on electrons, exemplified by the spin-orbit coupling, mingle the spin and orbital degrees of freedom and bring the interplay between electric and magnetic properties. Multiferroics is a manifestation in insulators, where a magnetization induces an electric polarization and vice versa [1–4]. In metals and semiconductors, the spin-orbit coupling enables control of electrons' spin from electric current, and it is essential for spintronics. For example, the Rashba spin-orbit coupling causes the Edelstein effect [5], which produces spin polarization by electric current in inversion-breaking systems. Spintronics conventionally utilizes ferromagnets. Antiferromagnetic spintronics recently has gained more interest owing to various advantages such as fast response, no stray field, and large magnetotransport effects [6–8]. However, because the net magnetization vanishes in an antiferromagnet, manipulation and detection remain essential challenges.

A magnetization pattern in general configures a spiral order with strong correlation or with magnetic elements with a fixed magnetic moment. Magnetism breaks time-reversal symmetry $\mathcal{T}$ even though a spiral magnetic order may have no net magnetic moment. In addition, a spiral order is characterized by a wave vector $\boldsymbol{Q}$ and often breaks inversion symmetry $\mathcal{P}$ regardless of the underlying crystalline symmetry.

We study various phenomena related to broken $\mathcal{T}$ and $\mathcal{P}$ symmetries in magnetic Dirac materials in a unified fashion. The spin-orbit coupling naturally arises from the Dirac equation; as it abides by relativity, the coupling between the electric and magnetic degrees of freedom is contained. There are various materials where the Dirac Hamiltonian becomes the effective model near the chemical potential. Examples are the three-dimensional topological insulators (TIs) Bi_2Se_3 and Bi_2Te_3 [9–14]. With an insulating bulk, the topologically protected surface states determine the physical properties, which have been extensively studied [15,16]. In the doped case, however, the bulk states dominate the electric and magnetic properties of the system. When a magnetic order is present, the bulk of TIs offer an ideal laboratory to study the Dirac electrons with the exchange coupling to the magnetic moments.

In this Letter, we consider the electromagnetic response of a gapped Dirac system coupled to local magnetic moments. Our model describes the magnetically doped TIs Bi_2Se_3 and Bi_2Te_3 [17–21], where the magnetic dopants couple locally to the Dirac electrons via the exchange coupling. We first show that an inversion-breaking magnetic order can generate a finite electric polarization in the insulating state while the pristine electronic system is centrosymmetric. In a doped metallic state, we reveal that a magnetic order can induce anisotropic resistance. In addition, an electric field produces a uniform magnetization and in reverse an oscillating magnetic order generates direct current. We also discuss the
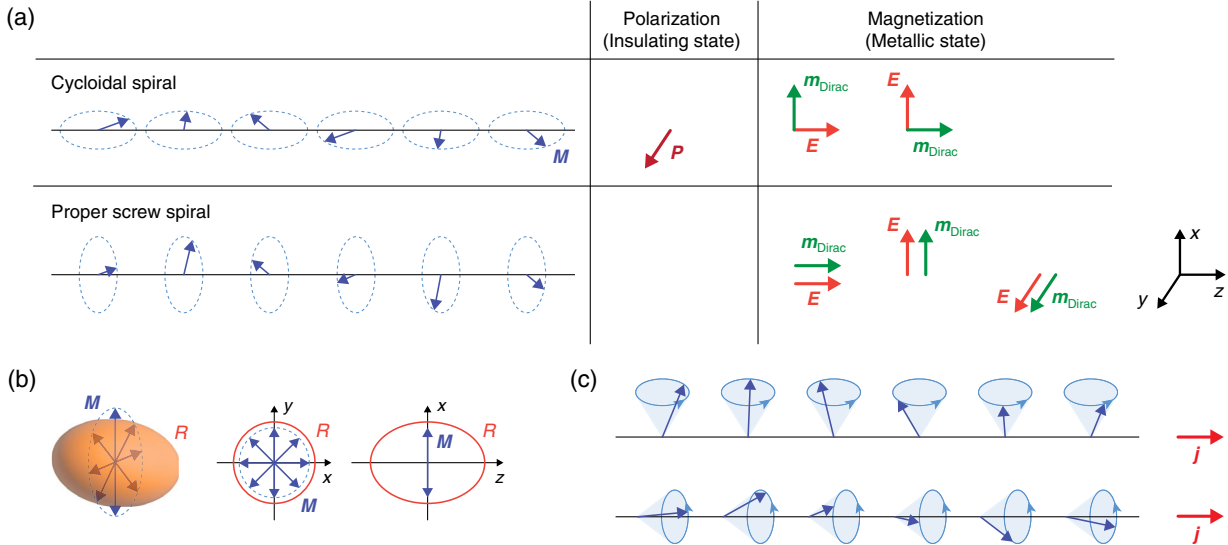
FIG. 1. Electromagnetic properties of a magnetic TI. (a) Polarization in the insulating state and magnetization in the metallic state induced by cycloidal and proper screw spiral magnetic orders. With the wave vector $\boldsymbol{Q}\|\hat{z}$, the cycloidal spiral order is characterized by $\boldsymbol{M_Q} \propto \hat{y} - i\hat{z}$ and the proper screw spiral order by $\boldsymbol{M_Q} \propto \hat{x} - i\hat{y}$. For those two spiral orders, only the cycloidal order displays a finite polarization according to Eq. (3). In the metallic state, the induced magnetization of the Dirac electrons $\boldsymbol{m}_{\mathrm{Dirac}}$ varies with the electric field; see Eq. (8). (b) Anisotropic magnetoresistance in the presence of a spiral magnetic order Eq. (7). The left panel is a three-dimensional illustration of the anisotropic resistance R, and the center and right panels are the two distinct plane cuts, displaying the anisotropy in the plane perpendicular to the local magnetic moments. (c) Uniform direct current induced by oscillating magnetic orders. For oscillations forming cycloidal and proper screw patterns, the generated direct current is parallel to the wave vector of the magnetic orders, following Eq. (9).

intrinsic magnetic TI MnBi$_2$Te$_4$ [22–25] and the possibility of inversion-breaking magnetic orders in magnetic TIs.

Model.—We consider a three-dimensional isotropic gapped Dirac system. Such an electronic system is realized, for example, in the bulk of TIs. For the TIs Bi$_2$Se$_3$ and Bi$_2$Te$_3$, the energy bands near the Γ point describe the low-energy behavior, which consists of the spin $\boldsymbol{\sigma}$ and p orbitals $\boldsymbol{\tau}$ from Bi ($\tau_z = +1$) and Se/Te ($\tau_z = -1$). To linear order in momentum $\boldsymbol{k}$, the $\boldsymbol{k} \cdot \boldsymbol{p}$ Hamiltonian becomes

$$H_0(\boldsymbol{k}) = m\beta + \boldsymbol{\alpha} \cdot \boldsymbol{k}, \tag{1}$$

where the 4×4 matrices $\boldsymbol{\alpha} = \boldsymbol{\sigma}\tau_x$ and $\beta = \tau_z$ satisfy the anticommutation relations $\{\alpha_a, \alpha_b\} = \{\alpha_a, \beta\} = 0 \ (a \neq b)$ and $\alpha_a^2 = \beta^2 = I$ (I: identity matrix) [10]. We set $\hbar = 1$. The pristine system preserves inversion $\mathcal{P} = \tau_z$ and time reversal $\mathcal{T} = i\sigma_y \mathcal{K}$ with the complex conjugate operator $\mathcal{K}$: $\mathcal{P}H_0(\boldsymbol{k})\mathcal{P}^{-1} = H_0(-\boldsymbol{k})$ and $\mathcal{T}H_0(\boldsymbol{k})\mathcal{T}^{-1} = H_0(-\boldsymbol{k})$. The kinetic term renders the spin and orbital coupling, so that neither is a good quantum number. The sign of the mass can be either positive or negative, which describes the band inversion near the Γ point.

Magnetic dopants such as Mn, Cr, and Fe can substitute the Bi sites of Bi$_2$Se$_3$ and Bi$_2$Te$_3$ [26]. Their local magnetic moments break time-reversal symmetry and tend to form a magnetic order. In a metallic state, the Ruderman-Kittel-Kasuya-Yosida (RKKY) interaction favors ferromagnetism when the Fermi level is near the Dirac point, but in general a complex magnetic order may occur depending on the Fermi

level, anisotropy, and inhomogeneity [27–30]. An effective spin Hamiltonian reflecting such details of the system determines the magnetic order $\boldsymbol{M}(\boldsymbol{r}) = \sum_{\boldsymbol{Q}} \boldsymbol{M_Q} e^{i\boldsymbol{Q} \cdot \boldsymbol{r}}$, which we take as given in the following analyses.

The exchange coupling yields the local magnetic coupling to the Dirac electrons. We note that the exchange coupling is orbital dependent [31]:

$$H'(\boldsymbol{r}) = -J\boldsymbol{M}(\boldsymbol{r}) \cdot \boldsymbol{\sigma} - J'\tilde{\beta}\boldsymbol{M}(\boldsymbol{r}) \cdot \boldsymbol{\sigma}. \tag{2}$$

Here, we introduce $\tilde{\beta} = \tau_z \mathrm{sgn}(m)$ for later convenience. The two coupling constants J and J' describe the different strengths of the exchange coupling for the two orbitals ($\tau_z = \pm 1$).

Insulating state.—The bulk is insulating when the chemical potential lies inside the mass gap. While the electronic system preserves inversion, the magnetic order may violate it, allowing a finite electric polarization. The calculation of the polarization follows the method by King-Smith and Vanderbilt [32]. We find an inversion-breaking magnetic order produces a finite polarization of the Dirac electrons

$$\Delta\boldsymbol{P} = -\frac{eJJ'}{6\pi^2|m|}\sum_{\boldsymbol{Q}}\mathrm{Im}[\boldsymbol{M_Q^*}(\boldsymbol{Q} \cdot \boldsymbol{M_Q})]; \tag{3}$$

see Supplemental Material (SM) for details [33].

The result conforms to the analyses of a Ginzburg-Landau model [34] and a microscopic model [35], where certain chiral magnetic orders induce a finite electric polarization. For cycloidal and proper screw orders, only the former induce a finite polarization perpendicular to the wave vector in the magnetization plane according to Eq. (3) [Fig. 1(a)]. The product JJ' implies that the strengths of the exchange coupling should be different for the two orbitals for a finite polarization. The orbital-dependent exchange coupling mixes the conduction and valence bands by the magnetic order to realize a finite polarization.

Effective Hamiltonian in the metallic state.—When the system is metallic, we expect various responses to an external electromagnetic field. As charges in the vicinity of the Fermi surface are dominantly responsible to electromagnetic response, it is convenient to derive the effective Hamiltonian for the bands that cross the Fermi energy. We obtain the effective Hamiltonian by following the method by Foldy and Wouthuysen [40], and Tani [41], which we can calculate as a perturbative series in the large mass limit $|m| \gg |\epsilon_F|$ (ϵ_F: the Fermi energy measured from a band edge) [33]. In the presence of an external electromagnetic field, the effective Hamiltonian to order m^{-2} is

$$
\begin{aligned}
H_{\text{eff}} = {} & |m|\tilde{\beta} - e\Phi - (J + J'\tilde{\beta})\boldsymbol{M}\cdot\boldsymbol{\sigma} + \frac{\tilde{\beta}}{2|m|}(\boldsymbol{\Pi}\cdot\boldsymbol{\Pi} + e\boldsymbol{\sigma}\cdot\boldsymbol{B}) + \frac{e}{8m^2}(\nabla\cdot\boldsymbol{E}) + \frac{e}{8m^2}[\boldsymbol{\Pi}\cdot(\boldsymbol{\sigma}\times\boldsymbol{E}) + (\boldsymbol{\sigma}\times\boldsymbol{E})\cdot\boldsymbol{\Pi}] \\
& + \frac{J}{8m^2}\{(\boldsymbol{\Pi}\cdot\boldsymbol{\sigma})[-i\nabla\cdot\boldsymbol{M} + \boldsymbol{\sigma}\cdot(\nabla\times\boldsymbol{M}) - 2i(\boldsymbol{\sigma}\times\boldsymbol{M})\cdot\boldsymbol{\Pi}] + \text{H.c.}\} \\
& + \frac{J'\tilde{\beta}}{8m^2}\{(\boldsymbol{\Pi}\cdot\boldsymbol{\sigma})[-i\nabla\cdot\boldsymbol{M} + \boldsymbol{\sigma}\cdot(\nabla\times\boldsymbol{M}) + 2\boldsymbol{M}\cdot\boldsymbol{\Pi}] + \text{H.c.}\},
\end{aligned} \tag{4}
$$

with $\boldsymbol{\Pi} = \boldsymbol{p} + e\boldsymbol{A}$ and the momentum operator $\boldsymbol{p} = -i\nabla$. The charge of an electrons is $-e$. The electric and magnetic fields are $\boldsymbol{E} = -\nabla\Phi - \partial\boldsymbol{A}/\partial t$ and $\boldsymbol{B} = \nabla\times\boldsymbol{A}$, respectively, with the scalar potential Φ and the vector potential $\boldsymbol{A}$. In the effective Hamiltonian, $\tilde{\beta} = \pm 1$ signifies the energy bands: $\tilde{\beta} = +1$ corresponds to the conduction band and $\tilde{\beta} = -1$ to the valence band. Although we originally define $\tilde{\beta} = \tau_z\text{sgn}(m)$, it does not precisely label the orbitals after the unitary transformation.

The last two terms of the effective Hamiltonian (4) reveal the nontrivial coupling between the Dirac electrons and the magnetic order, which is central to the following results. It manifests the strong spin-orbital coupling embedded in the Dirac Hamiltonian along with the exchange coupling. It also modifies the current density operator $\mathcal{J} = ie[\boldsymbol{r}, H_{\text{eff}}]$ to become

$$
\begin{aligned}
\mathcal{J} = {} & -\frac{e}{m}\beta\boldsymbol{p} - \frac{e}{4m^2}(J + J'\beta)(\nabla\times\boldsymbol{M}) \\
& - \frac{e}{4m^2}\{J[-2i\boldsymbol{M}\times\boldsymbol{p} - \boldsymbol{\sigma}\times(\boldsymbol{M}\times\boldsymbol{p}) - \boldsymbol{M}\times(\boldsymbol{\sigma}\times\boldsymbol{p})] \\
& + J'\tilde{\beta}[\boldsymbol{\sigma}(\boldsymbol{M}\cdot\boldsymbol{p}) + \boldsymbol{M}(\boldsymbol{\sigma}\cdot\boldsymbol{p})] + \text{H.c.}\}
\end{aligned} \tag{5}
$$

at zero frequency. The second term with $\nabla\times\boldsymbol{M}$ has a classical analog to the Ampère's circuital law. The third term contains the local magnetic moment $\boldsymbol{M}$ and the spin of the Dirac electrons $\boldsymbol{\sigma}$. It implies the possibility of the mutual control of the electric and magnetic degrees of freedom as we will see below.

Current under an electric field.—We perform perturbative calculations using functional derivatives to calculate response. We define the action $S = T\sum_{\omega_n}\int d\boldsymbol{r}\bar{\psi}(-i\omega_n + H_{\text{eff}})\psi$, where T is the temperature and $\omega_n = (2n+1)\pi T$ is the fermionic Matsubara frequency. Using the partition function $Z = \int D\bar{\psi}D\psi e^{-S}$, we obtain the current response in the presence of an external electric field $\boldsymbol{E}(\omega) = i\omega\boldsymbol{A}(\omega)$ ($\Phi = 0$) as

$$
j_a(\omega) = \langle\hat{j}_a(\omega)\rangle = \frac{1}{i\omega}\frac{\delta^2\ln Z}{\delta A_a(-\omega)\delta A_b(\omega)}\bigg|_{E=0}E_b(\omega). \tag{6}
$$

We note that it is equivalent to the Kubo formula. We calculate it perturbatively with respect to the exchange couplings J, J', and the inverse mass m^{-1}, using the unperturbed Green's function $G_0 = (\omega - H_{\text{eff}}^0 - \Sigma)^{-1}$ with $H_{\text{eff}}^0 = m\beta + \beta k^2/(2m)$ and the self-energy Σ. We approximate $\Sigma \approx -i\text{sgn}(\omega_n)/(2\tau)$ with a constant τ to describe momentum relaxation in diffusive transport.

The magnetic order alters the current flow. When we focus on a spatially uniform current, the lowest-order corrections by the magnetic order appear as a product of $\boldsymbol{M_Q}$ and $\boldsymbol{M_Q^*}$. By differentiating Eq. (6) with respect to $\boldsymbol{M_Q}$ and $\boldsymbol{M_Q^*}$, we obtain the conductivity tensor

$$
\begin{aligned}
\sigma_{ab}(\omega) = {} & \sigma_0(\omega)\delta_{ab} + \sigma_{ab}^{\text{AH}}(\omega) - \eta(\omega)\sum_{\boldsymbol{Q}}|\boldsymbol{M_Q}|^2\delta_{ab} \\
& + \eta'(\omega)\sum_{\boldsymbol{Q}}(M_{\boldsymbol{Q},a}^*M_{\boldsymbol{Q},b} + M_{\boldsymbol{Q},a}M_{\boldsymbol{Q},b}^*),
\end{aligned} \tag{7}
$$

where the coefficients are given by

$$\sigma_0(\omega) = \frac{e^2|n(\epsilon_F)|\tau_\omega}{|m|},$$

$$\eta(\omega) = \frac{2e^2|n(\epsilon_F)|\tau_\omega^3}{|m|}(J + J'\tilde{\beta})^2,$$

$$\eta'(\omega) = \frac{e^2|n(\epsilon_F)|\tau_\omega}{8|m|^3}(-3J^2 + 5J'^2 - 2JJ'\tilde{\beta}).$$

$n(\epsilon_F) \propto |\epsilon_F|^{3/2}$ is the carrier density ($n > 0$ for electrons and $n < 0$ for holes). We introduce $\tau_\omega = \tau/(1 - i\omega\tau)$ and retain the leading-order contributions in m^{-1} in the expressions of σ, η, and η'. When there is a uniform magnetization $\mathbf{M_0} \neq \mathbf{0}$, it yields the anomalous Hall contribution $\sigma_{ab}^{\mathrm{AH}} \propto \varepsilon_{abc}M_{\mathbf{0},c}$; see SM for details [33]. $\mathbf{j}(\omega)$ depends only on $\mathbf{M_Q}$ but does not directly depend on $\mathbf{Q}$ to this order.

The spatial pattern of the magnetic order modifies the conductivity at second order in $\mathbf{M}$. The first correction with $\eta(\omega)$ reduces the longitudinal conductivity, arising from the exchange coupling $-(J + J'\tilde{\beta})\mathbf{M} \cdot \boldsymbol{\sigma}$. The effect is isotropic and it does not require the spin-orbital coupling inherent in the Dirac Hamiltonian. It resembles the magnetoresistance whereas there is no uniform magnetization by assumption. On the other hand, the η' term can be traced to the coupling between the magnetic order and current, as we have seen in Eq. (5). It gives rise to anisotropic corrections to the conductivity tensor $\sigma_{ab}(\omega)$ depending on the magnetic order.

The second-order corrections to the conductivity correspond to the anisotropic magnetoresistance and the planar Hall effect [42]. Both cycloidal and screw magnetic orders show the anisotropic resistance R [Fig. 1(b)]: when the magnetic order lies in the xy plane, the resistance is different in the xy plane and along the z axis. We emphasize, however, that the second-order effect in Eq. (7) appears even without a uniform magnetization. Therefore, when there is no uniform magnetization, namely, $\sigma_{ab}^{\mathrm{AH}} = 0$, the conductivity tensor is symmetric: $\sigma_{ab}(\omega) = \sigma_{ba}(\omega)$. On the other hand, the anomalous Hall contribution is antisymmetric: $\sigma_{ab}^{\mathrm{AH}}(\omega) = -\sigma_{ba}^{\mathrm{AH}}(\omega)$ [43].

Magnetization by an electric field.—From the coupling between the current and the spin degrees of freedom, we expect that an electric field produces a finite magnetization of Dirac electrons even when the magnetic order has no uniform magnetization. We evaluate the spin expectation value of the Dirac electrons $\langle\boldsymbol{\sigma}\rangle$ in the presence of an external electric field $\mathbf{E}$ and the magnetic order $\mathbf{M}$ using H_{eff}. The uniform magnetization of the Dirac electrons is given by $\mathbf{m}_{\mathrm{Dirac}} = -g\mu_B\langle\boldsymbol{\sigma}\rangle/2$, where g is the g factor and μ_B is the Bohr magneton. A perturbative calculation finds a finite magnetization under a static and uniform external electric field [33]

$$\mathbf{m}_{\mathrm{Dirac}} = \lambda^{(1)}\sum_{\mathbf{Q}}(\mathbf{Q} \cdot \mathbf{E})\mathrm{Im}(\mathbf{M_Q} \times \mathbf{M_Q^*})$$

$$+ \lambda^{(2)}\sum_{\mathbf{Q}}\{\mathrm{Im}[(\mathbf{M_Q^*} \times \mathbf{Q})(\mathbf{M_Q} \cdot \mathbf{E})]$$

$$+ \mathrm{Im}[(\mathbf{M_Q^*} \times \mathbf{E})(\mathbf{Q} \cdot \mathbf{M_Q})]\} \quad (8)$$

with

$$\lambda^{(1)} = \frac{g\mu_B en(\epsilon_F)}{m^2}\tau^3 J(J + J'\tilde{\beta}),$$

$$\lambda^{(2)} = \frac{g\mu_B en(\epsilon_F)}{2m^2}\tau^3(J^2 - J'^2).$$

Since the magnetization and the electric field transforms differently under inversion, an inversion-breaking magnetic order is necessary to induce magnetization by an electric field [Fig. 1(a)]. It allows detection of an inversion-breaking magnetic order through the magnetization by applying an electric field. The change of the magnetization under an electric field can be attributed to $\mathbf{m}_{\mathrm{Dirac}}$. The effect resembles the Edelstein effect but it appears in the bulk of a TI, where inversion is broken by a magnetic order. The extension to a time-dependence case is straightforward [33].

Current by an oscillating magnetic order.—We now investigate whether an external magnetic field induces an electric current. The magnetic field should vary in time as a spatially uniform current cannot exist in the equilibrium. The external magnetic field applied to a metallic system with a magnetic order has the following two effects: it couples to the itinerant electrons to induce cyclotron motion; at the same time, it drives the Rabi oscillation and the Larmor precession of the local magnetic moments.

We first check if a uniform oscillating magnetic field $\mathbf{B}(\omega)$ induces a uniform current in the presence of a static magnetic order. From the symmetry consideration, the lowest-order contribution should have the form $j_a(\omega) = \kappa_{abcd}B_b(\omega)M_{\mathbf{Q},c}M_{-\mathbf{Q},d}$ with κ_{abcd} linear in $\mathbf{Q}$. However, this mechanism is improbable. The conductivity tensor Eq. (7) is insensitive to inversion breaking, so that the cyclotron motion of the Dirac electrons would not yield a uniform current. We calculate κ_{ijkl} perturbatively and observe that it vanishes to order $QJ^2n(\epsilon_F)/m^2$ [33].

We then examine current response by an oscillating magnetic order. If it is finite, an external magnetic field induces an electric current by making the local magnetic moments oscillate. We write the spatial and temporal dependence of the magnetic order as $\mathbf{M}(\mathbf{r}, t) = \sum_{\mathbf{Q}\omega}\mathbf{M_{Q\omega}}e^{i(\mathbf{Q}\cdot\mathbf{r}-\omega t)}$. Here, we seek the uniform current response of the form $j_a(\omega_1 + \omega_2) = \gamma_{abc}(\omega_1, \omega_2, \mathbf{Q})M_{\mathbf{Q}\omega_1,b}M_{-\mathbf{Q}\omega_2,c}$, where γ_{abc} is linear in the wave vector $\mathbf{Q}$ to capture the inversion breaking by the magnetic order and hence to comply with the symmetry constraint. As a second-order response, the output frequency

is the sum of two input frequencies. We can calculate the current response similarly to $\sigma_{ab}(\omega)$ [33]:

$$
\begin{aligned}
\boldsymbol{j}(\omega) = \sum_{\boldsymbol{Q}\omega_1\omega_2} \delta_{\omega_1+\omega_2,\omega}[&\gamma^{(S)}(\omega_1,\omega_2)\boldsymbol{Q}\times(\boldsymbol{M}_1\times\boldsymbol{M}_2) \\
&+ \gamma^{(A)}(\omega_1,\omega_2) \\
&\times \{J[\boldsymbol{M}_1\times(\boldsymbol{Q}\times\boldsymbol{M}_2)+\boldsymbol{M}_2\times(\boldsymbol{Q}\times\boldsymbol{M}_1)] \\
&+ J'\tilde{\beta}[\boldsymbol{M}_1(\boldsymbol{Q}\cdot\boldsymbol{M}_2)+\boldsymbol{M}_2(\boldsymbol{Q}\cdot\boldsymbol{M}_1)]\}],
\end{aligned}
\tag{9}
$$

where we denote $\boldsymbol{M}_1 = \boldsymbol{M}_{\boldsymbol{Q}\omega_1}$, $\boldsymbol{M}_2 = \boldsymbol{M}_{-\boldsymbol{Q}\omega_2}$, and the coefficients are

$$
\begin{aligned}
\gamma^{(S)}(\omega_1,\omega_2) = \frac{e}{8m^2}&n(\epsilon_F)(J+J'\tilde{\beta})^2 \\
&\times i(\omega_1+\omega_2)\tau_{\omega_1+\omega_2}(\omega_1\tau_{\omega_1}^2+\omega_2\tau_{\omega_2}^2),
\end{aligned}
$$

$$
\gamma^{(A)}(\omega_1,\omega_2) = -\frac{e}{4m^2}(J+J'\tilde{\beta})n(\epsilon_F)(\omega_1\tau_{\omega_1}^2-\omega_2\tau_{\omega_2}^2).
$$

$\gamma^{(S)}(\omega_1,\omega_2)$ and $\gamma^{(A)}(\omega_1,\omega_2)$ are symmetric and antisymmetric under the exchange of ω_1 and ω_2, respectively. $\gamma^{(A)}(\omega,-\omega)$ corresponds to zero-frequency response, namely direct current depicted in Fig. 1(c), and $\gamma^{(S)}(\omega,\omega)$ to 2ω response.

It is worth contrasting the current response in the metallic state (9) with the polarization in the insulating state (3) as they reflect different material properties. First, the current response requires dynamics of the magnetic order whereas the polarization is a thermodynamic quantity defined in the equilibrium. The diffusive nature of the current is manifested in the appearance of the lifetime τ. Second, the current is carried by electric charges near the Fermi energy and it is thus proportional to the carrier density. On the other hand, the polarization only involves the quantities that characterize the system, implying that it requires the information of the entire band structure. Indeed, we cannot obtain Eq. (3) from the effective Hamiltonian (4) but from the original model (1).

As we have discussed, the local magnetic moments oscillate under a time-dependent external magnetic field to induce a uniform electric current. When the oscillation is near resonance, we may expect a larger current response. Since it is a second-order response with respect to the magnetic order, the response should be peaked at the zero frequency and double the resonance frequency. A magnetic order might also be driven by the spin wave spectroscopy technique [44–46]. An oscillating magnetic field is induced by periodically aligned wave guides whereby the wave vector of the magnetic field is designed.

Discussions.—We have revealed that electromagnetic response of a magnetic TI manifests the entanglement of the spin and orbital degrees of freedom and hence the electric and magnetic properties. Particularly with an inversion-breaking magnetic order, it allows a measurement of electric properties through a magnetic probe and vice versa, and suggest applications in spintronics.

In addition to the magnetically doped TIs, we can consider the stoichiometric magnetic TI MnBi$_2$Te$_4$. It consists of stacking layers of TI films, bound by the van der Waals interaction [22]. The low-energy effective Hamiltonian is $H_{\mathrm{STI}}(\boldsymbol{k}) = m\tau_x + v\tau_z(\hat{z}\times\boldsymbol{\sigma})\cdot\boldsymbol{k}_\perp + v_z k_z\tau_y$, where the stacking direction is set along the z direction and τ_z corresponds to the top and bottom TI surface states of a constituent layer [36]. In SM [33], we confirm that an inversion-breaking magnetic order induces an electric polarization in the insulating state, and derive the effective Hamiltonian for the metallic case to see that the current operator is affected by the magnetic order.

Experimentally, a spiral magnetic order has not yet been reported in magnetic TIs, but yet some experiments reveal noncollinear magnetic orders. Stacking layers of MnBi$_2$Te$_4$ realize a canted antiferromagnetic order [47], and alternating stacks of MnBi$_2$Te$_4$ and Bi$_2$Te$_3$ lead to a variety of heterostructures $(\mathrm{MnBi}_2\mathrm{Te}_4)_m(\mathrm{Bi}_2\mathrm{Te}_3)_n$ [48]. The topological Hall effect is observed in the magnetic and nonmagnetic topological insulator heterostructures $\mathrm{Cr}_x(\mathrm{Bi}_{1-y}\mathrm{Sb}_y)_{2-x}\mathrm{Te}_3/(\mathrm{Bi}_{1-y}\mathrm{Sb}_y)_2\mathrm{Te}_3$ and a theory attributed its origin to a Néel-type skyrmion, consisting of the superposition of the local three spiral orders [37]. The topological Hall effect attributed to skyrmions is also observed in Mn-doped Bi$_2$Te$_3$ topological insulator films [49]. Those observations suggest that various magnetic orders may appear by different stacks and material compositions.

We now estimate the magnitude of the effects that we have discussed using the material parameters of $\mathrm{Cr}_x(\mathrm{Bi}_{1-y}\mathrm{Sb}_y)_{2-x}\mathrm{Te}_3$ [37]: $m = -300$ meV, $J = -5$ meV, $J' = 1$ meV, and the velocity $v = 5.0\times10^5$ m/s; see SM for details [33]. The magnetic moment per Cr atom is $M \approx 3\mu_B$. We set $\epsilon_F = -100$ meV. The RKKY interaction would form a magnetic order in the metallic state with the wave number $Q = 2k_F \approx 1.5\times10^9$ m^{-1}. We estimate $\tau \approx 5\times10^{-15}$ s from the longitudinal conductivity 100 Ω^{-1} cm^{-1} with $|n| \approx 1.4\times10^{19}$ cm^{-3}. Then, the corrections to the conductivity are $-2\eta M^2 \approx -8.7$ Ω^{-1} cm^{-1} and $4\eta'M^2 \approx -0.4$ Ω^{-1} cm^{-1} for the isotropic and anisotropic parts, respectively. The magnetization induced by the current density $j = 10^8$ A/m is $m_{\mathrm{Dirac}} \sim 10^{-4}$ A/m. The current densities generated by an oscillating magnetic order at 1 GHz are $\gamma^{(S)}QM^2 \approx 9.2$ A/m^2 for the sum frequency generation and $\gamma^{(A)}JQM^2 \approx -2.3\times10^5$ A/m^2. We note that the former grows quadratically with frequency while the latter does linearly. In the insulating state, the electric polarization is $\Delta P \approx 1.8$ µC/m^2 with the same Q. From those estimates, the electronic response is more likely to be observable that the magnetic one.

In addition to magnetic TIs, we also anticipate similar current response in magnetic Weyl and Dirac semimetals, where an emergent electromagnetic field plays a role as

well as the Berry curvature [50–52]. A surface, an interface, and a domain wall geometrically break inversion, and thus the existence of a magnetic order can also induce various response. Such structures without inversion support the Dzyaloshinskii-Moriya interaction, which could contribute to a chiral magnetic order to reveal the effects that we have discussed.

[1] T. Kimura, Spiral magnets as magnetoelectrics, Annu. Rev. Mater. Res. **37**, 387 (2007).

[2] Y. Tokura, S. Seki, and N. Nagaosa, Multiferroics of spin origin, Rep. Prog. Phys. **77**, 076501 (2014).

[3] M. Fiebig, T. Lottermoser, D. Meier, and M. Trassin, The evolution of multiferroics, Nat. Rev. Mater. **1**, 16046 (2016).

[4] N. A. Spaldin and R. Ramesh, Advances in magnetoelectric multiferroics, Nat. Mater. **18**, 203 (2019).

[5] V. M. Edelstein, Spin polarization of conduction electrons induced by electric current in two-dimensional asymmetric electron systems, Solid State Commun. **73**, 233 (1990).

[6] T. Jungwirth, X. Marti, P. Wadley, and J. Wunderlich, Antiferromagnetic spintronics, Nat. Nanotechnol. **11**, 231 (2016).

[7] O. Gomonay, T. Jungwirth, and J. Sinova, Concepts of antiferromagnetic spintronics, Phys. Status Solidi RRL **11**, 1700022 (2017).

[8] V. Baltz, A. Manchon, M. Tsoi, T. Moriyama, T. Ono, and Y. Tserkovnyak, Antiferromagnetic spintronics, Rev. Mod. Phys. **90**, 015005 (2018).

[9] Y. Xia, D. Qian, D. Hsieh, L. Wray, A. Pal, H. Lin, A. Bansil, D. Grauer, Y. S. Hor, R. J. Cava, and M. Z. Hasan, Observation of a large-gap topological-insulator class with a single Dirac cone on the surface, Nat. Phys. **5**, 398 (2009).

[10] H. Zhang, C.-X. Liu, X.-L. Qi, X. Dai, Z. Fang, and S.-C. Zhang, Topological insulators in Bi_2Se_3, Bi_2Te_3 and Sb_2Te_3 with a single Dirac cone on the surface, Nat. Phys. **5**, 438 (2009).

[11] J. Moore, The next generation, Nat. Phys. **5**, 378 (2009).

[12] Y. L. Chen, J. G. Analytis, J.-H. Chu, Z. K. Liu, S.-K. Mo, X. L. Qi, H. J. Zhang, D. H. Lu, X. Dai, Z. Fang, S. C. Zhang, I. R. Fisher, Z. Hussain, and Z.-X. Shen, Experimental realization of a three-dimensional topological insulator, Bi_2Te_3, Science **325**, 178 (2009).

[13] D. Hsieh, Y. Xia, D. Qian, L. Wray, J. H. Dil, F. Meier, J. Osterwalder, L. Patthey, J. G. Checkelsky, N. P. Ong, A. V. Fedorov, H. Lin, A. Bansil, D. Grauer, Y. S. Hor, R. J. Cava, and M. Z. Hasan, A tunable topological insulator in the spin helical Dirac transport regime, Nature (London) **460**, 1101 (2009).

[14] Y. S. Hor, A. Richardella, P. Roushan, Y. Xia, J. G. Checkelsky, A. Yazdani, M. Z. Hasan, N. P. Ong, and R. J. Cava, p-type Bi_2Se_3 for topological insulator and low-temperature thermoelectric applications, Phys. Rev. B **79**, 195208 (2009).

[15] M. Z. Hasan and C. L. Kane, Colloquium: Topological insulators, Rev. Mod. Phys. **82**, 3045 (2010).

[16] X.-L. Qi and S.-C. Zhang, Topological insulators and superconductors, Rev. Mod. Phys. **83**, 1057 (2011).

[17] Y. S. Hor, P. Roushan, H. Beidenkopf, J. Seo, D. Qu, J. G. Checkelsky, L. A. Wray, D. Hsieh, Y. Xia, S.-Y. Xu, D. Qian, M. Z. Hasan, N. P. Ong, A. Yazdani, and R. J. Cava, Development of ferromagnetism in the doped topological insulator $Bi_{2-x}Mn_xTe_3$, Phys. Rev. B **81**, 195203 (2010).

[18] Y. L. Chen, J.-H. Chu, J. G. Analytis, Z. K. Liu, K. Igarashi, H.-H. Kuo, X. L. Qi, S. K. Mo, R. G. Moore, D. H. Lu, M. Hashimoto, T. Sasagawa, S. C. Zhang, I. R. Fisher, Z. Hussain, and Z. X. Shen, Massive Dirac fermion on the surface of a magnetically doped topological insulator, Science **329**, 659 (2010).

[19] L. A. Wray, S.-Y. Xu, Y. Xia, D. Hsieh, A. V. Fedorov, Y. S. Hor, R. J. Cava, A. Bansil, H. Lin, and M. Z. Hasan, A topological insulator surface under strong Coulomb, magnetic and disorder perturbations, Nat. Phys. **7**, 32 (2011).

[20] Y. Okada, C. Dhital, W. Zhou, E. D. Huemiller, H. Lin, S. Basak, A. Bansil, Y.-B. Huang, H. Ding, Z. Wang, S. D. Wilson, and V. Madhavan, Direct Observation of Broken Time-Reversal Symmetry on the Surface of a Magnetically Doped Topological Insulator, Phys. Rev. Lett. **106**, 206805 (2011).

[21] J. Zhang, C.-Z. Chang, P. Tang, Z. Zhang, X. Feng, K. Li, L.-l. Wang, X. Chen, C. Liu, W. Duan, K. He, Q.-K. Xue, X. Ma, and Y. Wang, Topology-driven magnetic quantum phase transition in topological insulators, Science **339**, 1582 (2013).

[22] M. M. Otrokov et al., Prediction and observation of an antiferromagnetic topological insulator, Nature (London) **576**, 416 (2019).

[23] I. I. Klimovskikh et al., Tunable 3D/2D magnetism in the $(MnBi_2Te_4)(Bi_2Te_3)_m$ topological insulators family, npj Quantum Mater. **5**, 54 (2020).

[24] B. Li, J.-Q. Yan, D. M. Pajerowski, E. Gordon, A.-M. Nedić, Y. Sizyuk, L. Ke, P. P. Orth, D. Vaknin, and R. J. McQueeney, Competing Magnetic Interactions in the Antiferromagnetic Topological Insulator $MnBi_2Te_4$, Phys. Rev. Lett. **124**, 167204 (2020).

[25] J. Li, Y. Li, S. Du, Z. Wang, B.-L. Gu, S.-C. Zhang, K. He, W. Duan, and Y. Xu, Intrinsic magnetic topological insulators in van der Waals layered $MnBi_2Te_4$-family materials, Sci. Adv. **5**, eaaw5685 (2019).

[26] Y. Tokura, K. Yasuda, and A. Tsukazaki, Magnetic topological insulators, Nat. Rev. Phys. **1**, 126 (2019).

[27] Q. Liu, C.-X. Liu, C. Xu, X.-L. Qi, and S.-C. Zhang, Magnetic Impurities on the Surface of a Topological Insulator, Phys. Rev. Lett. **102**, 156603 (2009).

[28] D. A. Abanin and D. A. Pesin, Ordering of Magnetic Impurities and Tunable Electronic Properties of Topological Insulators, Phys. Rev. Lett. **106**, 136802 (2011).

[29] A. W. Overhauser, Giant Spin Density Waves, Phys. Rev. Lett. **4**, 462 (1960).

[30] A. W. Overhauser, Spin density waves in an electron gas, Phys. Rev. **128**, 1437 (1962).

[31] R. Wakatsuki, M. Ezawa, and N. Nagaosa, Domain wall of a ferromagnet on a three-dimensional topological insulator, Sci. Rep. **5**, 13638 (2015).

[32] R. D. King-Smith and D. Vanderbilt, Theory of polarization of crystalline solids, Phys. Rev. B **47**, 1651 (1993).

[33] See Supplemental Material at http://link.aps.org/supplemental/10.1103/PhysRevLett.129.216601, which includes Refs. [10,31,32,34–39] for the details about the polarization, the unitary transformation, the calculations of response, and the material estimates.

[34] M. Mostovoy, Ferroelectricity in Spiral Magnets, Phys. Rev. Lett. **96**, 067601 (2006).

[35] H. Katsura, N. Nagaosa, and A. V. Balatsky, Spin Current and Magnetoelectric Effect in Noncollinear Magnets, Phys. Rev. Lett. **95**, 057205 (2005).

[36] C. Lei, S. Chen, and A. H. MacDonald, Magnetized topological insulator multilayers, Proc. Natl. Acad. Sci. U.S.A. **117**, 27224 (2020).

[37] K. Yasuda, R. Wakatsuki, T. Morimoto, R. Yoshimi, A. Tsukazaki, K. S. Takahashi, M. Ezawa, M. Kawasaki, N. Nagaosa, and Y. Tokura, Geometric Hall effects in topological insulator heterostructures, Nat. Phys. **12**, 555 (2016).

[38] Z. Wang, X.-L. Qi, and S.-C. Zhang, Topological Order Parameters for Interacting Topological Insulators, Phys. Rev. Lett. **105**, 256803 (2010).

[39] K.-T. Chen and P. A. Lee, Unified formalism for calculating polarization, magnetization, and more in a periodic insulator, Phys. Rev. B **84**, 205137 (2011).

[40] L. L. Foldy and S. A. Wouthuysen, On the Dirac theory of spin 1/2 particles and its nonrelativistic limit, Phys. Rev. **78**, 29 (1950).

[41] S. Tani, Connection between particle models and field theories, I: The case spin 1/2, Prog. Theor. Phys. **6**, 267 (1951).

[42] T. McGuire and R. Potter, Anisotropic magnetoresistance in ferromagnetic 3d alloys, IEEE Trans. Magn. **11**, 1018 (1975).

[43] N. Nagaosa, J. Sinova, S. Onoda, A. H. MacDonald, and N. P. Ong, Anomalous Hall effect, Rev. Mod. Phys. **82**, 1539 (2010).

[44] V. Vlaminck and M. Bailleul, Current-induced spin-wave Doppler shift, Science **322**, 410 (2008).

[45] V. Vlaminck and M. Bailleul, Spin-wave transduction at the submicrometer scale: Experiment and modeling, Phys. Rev. B **81**, 014425 (2010).

[46] S. Seki, Y. Okamura, K. Kondou, K. Shibata, M. Kubota, R. Takagi, F. Kagawa, M. Kawasaki, G. Tatara, Y. Otani, and Y. Tokura, Magnetochiral nonreciprocity of volume spin wave propagation in chiral-lattice ferromagnets, Phys. Rev. B **93**, 235131 (2016).

[47] D. Ovchinnikov, X. Huang, Z. Lin, Z. Fei, J. Cai, T. Song, M. He, Q. Jiang, C. Wang, H. Li, Y. Wang, Y. Wu, D. Xiao, J.-H. Chu, J. Yan, C.-Z. Chang, Y.-T. Cui, and X. Xu, Intertwined topological and magnetic orders in atomically thin Chern insulator $MnBi_2Te_4$, Nano Lett. **21**, 2544 (2021).

[48] J. Liu and T. Hesjedal, Magnetic topological insulator heterostructures: A review, Adv. Mater. 2102427 (2021). 10.1002/adma.202102427.

[49] C. Liu, Y. Zang, W. Ruan, Y. Gong, K. He, X. Ma, Q.-K. Xue, and Y. Wang, Dimensional Crossover-Induced Topological Hall Effect in a Magnetic Topological Insulator, Phys. Rev. Lett. **119**, 176809 (2017).

[50] J. Fröhlich and U. M. Studer, Gauge invariance and current algebra in nonrelativistic many-body theory, Rev. Mod. Phys. **65**, 733 (1993).

[51] B. W. A. Leurs, Z. Nazario, D. I. Santiago, and J. Zaanen, Non-Abelian hydrodynamics and the flow of spin in spin-orbit coupled substances, Ann. Phys. (Amsterdam) **323**, 907 (2008).

[52] Y. Araki, Magnetic textures and dynamics in magnetic Weyl semimetals, Ann. Phys. (Amsterdam) **532**, 1900287 (2020).